

NONLINEAR MOTIONS IN A HANGING CABLE

HYEYOUNG OH

ABSTRACT. We investigate the nonlinear motions of discrete loaded cable with different periodic forcing. We present the numerical evidence of the nonlinear motions of the cable by solving initial value problems and obtaining the motions after a long time. There appeared to be various types of nonlinear oscillations over a wide range of frequencies and amplitudes for the periodic forcing term.

1. Introduction

The original Tacoma Narrows Bridge, at all stages of its short life, was indeed very active in the wind. Its failure on 7 November 1940 attracted wide attention at the time and has elicited recurring references ever since, notably in physics, mathematics, and engineering [16].

The usual explanation says that the forcing term came from a train of alternating vortices being shed by the bridge as the wind blew past it. The frequency just happened to be at a value very close to a resonant frequency of the bridge. Thus, even though the magnitude of the forcing term was small, the phenomenon of linear resonance was enough to explain the large oscillation and eventual collapse of the bridge [10].

However, there still seems to be a need to give a clear mathematical argument as to why suspension bridges oscillate. As made clear in [1],

Received August 19, 2015. Revised October 28, 2015. Accepted October 30, 2015.
2010 Mathematics Subject Classification: 35G55, 35B05.

Key words and phrases: cable, nonlinear, node, multiple motions, asymmetric, initial value problem.

This work was supported by Incheon National University Research Grant in 2015.

© The Kangwon-Kyungki Mathematical Society, 2015.

This is an Open Access article distributed under the terms of the Creative Commons Attribution Non-Commercial License (<http://creativecommons.org/licenses/by-nc/3.0/>) which permits unrestricted non-commercial use, distribution and reproduction in any medium, provided the original work is properly cited.

[3], suspension bridges have a history of large-scale oscillation and catastrophic failure under high and even moderate winds, as well as under other mechanical forces.

What distinguished Tacoma Narrows was the extreme flexibility of its roadbed, being an order of magnitude higher than that of earlier bridges mentioned [1]. This resulted in a pronounced tendency to oscillate vertically, under widely differing wind conditions. The bridge might be quiet in winds of forty miles per hour, and might oscillate with large amplitude in winds as low as three or four miles per hour. These vertical oscillations were standing waves of different nodal types.

A pronounced torsional mode was observed just prior to the collapse of the bridge. This type of oscillation was observed after the bridge went into large vertical motion which apparently induced a slippage of a crucial part of the bridge called the cable band, which attached the center of the cable to the roadbed. Under the influence of the large amplitude vertical motions (of about five feet in amplitude with a frequency of 38 per minute), this band slipped, and “the change from the moderate parallel motions of the cables to the more violent out of phase motions was sudden” [10].

It should be noted that in the observed large-amplitude motion, some of the cables were alternately loosening and tightening. This is the non-linear effect. We can observe that the oscillations of cables in between transmission towers are distinctly different from that of a string under tension. As we shall see, there are large amplitude longitudinal motions under moderate small forcing amplitude. The resultant stresses can reach levels high enough to impair the safety of the towers so that such movements can cause the collapse of the transmission towers [12]. Such large amplitude motions cannot possibly be accounted by linear resonance as advocated by a number of elementary differential equation texts due to the precision of the wind force frequency required (a probability of 1 in 7200 is estimated on p.297,[4]). Unlike the linear resonance explanation, the same forcing term can give rise to a large or small periodic motion, with the result determined not by the forcing term, but by initial conditions.

We modelled a cable as a multiple particle oscillator and performed extensive numerical experiments.

We shall describe a variety of large-amplitude response to forcing term($f(\tilde{x}_i, t) = \lambda \sin 5\pi\tilde{x}_i \sin \mu t$). We find that multiple stable periodic

solutions exist under the periodic forcing. Some of these solutions possess large amplitudes and can be induced by proper initial conditions. A variety of different nodal structure of motions are appeared in our results, which observed prior to the failure of the Tacoma Narrows Bridge. In this study, we present the numerical evidence of the nonlinear motion of the cable by solving initial value problems.

2. Description of the hanging cable

In modelling the cable, we shall discretize what is essentially a continuous problem and shall use numerical computation to make some conclusions for the dynamical systems.

For this, we shall use the following. In 1744, Euler derived the correct equations for the large vibrations of a string in a plane. He regarded the equations as the limit of those for a finite collection of beads joined by massless springs as the number of beads approach infinity while their total mass remains fixed [2].

We shall solve the problem computationally for various different numbers of particles rather than follow Euler to the infinitesimal limit. And when we find that convergence is achieved, that is the behavior stays the same even as we increase the number of particles, then we believe that we have obtained a true solution of the mechanical system.

In this system, we shall consider the following:

- a cable suspended between two supports of equal elevation
- the gravitational load on the cable which keeps it in a state of tension near equilibrium
- some additional external forcing term due to some extraneous physical situation

We will treat a cable as a series of equally distributed point masses connected by nonlinear springs with the same unstretched lengths. To model the motion of the cable, the springs resist extension but compression. The restoring forces are presumed to be proportional to the extension (but not compression) of a one-sided spring joining two particles. Usually, they are subject to vertical periodic forces. Damping force will be assumed to act in a direction opposite to the motion with a magnitude proportional to the instantaneous velocity.

We consider a cable which is hung between two fixed points at the same vertical level and distance L apart. Let the line joining two supports be the x -axis with two fixed points located at $x = 0$ and $x = L$. Let the instantaneous position of the i -th particle be $(x_i(t), y_i(t))$ at time t with the positive directions for x and y . Then Newton's second law, Hooke's law, and the geometric relations between angles and lengths give rise to the following equations [13],

$$\begin{aligned} & \frac{d^2 x_i}{dt^2} \\ = & -\frac{k}{\rho l} (\sqrt{(x_i - x_{i-1})^2 + (y_i - y_{i-1})^2} - l)^+ \frac{(x_i - x_{i-1})}{\sqrt{(x_i - x_{i-1})^2 + (y_i - y_{i-1})^2}} \\ & + \frac{k}{\rho l} (\sqrt{(x_{i+1} - x_i)^2 + (y_{i+1} - y_i)^2} - l)^+ \frac{(x_{i+1} - x_i)}{\sqrt{(x_{i+1} - x_i)^2 + (y_{i+1} - y_i)^2}} \\ & - \frac{c}{\rho} dx_i/dt, \\ & \frac{d^2 y_i}{dt^2} \\ = & -\frac{k}{\rho l} (\sqrt{(x_i - x_{i-1})^2 + (y_i - y_{i-1})^2} - l)^+ \frac{(y_i - y_{i-1})}{\sqrt{(x_i - x_{i-1})^2 + (y_i - y_{i-1})^2}} \\ & + \frac{k}{\rho l} (\sqrt{(x_{i+1} - x_i)^2 + (y_{i+1} - y_i)^2} - l)^+ \frac{(y_{i+1} - y_i)}{\sqrt{(x_{i+1} - x_i)^2 + (y_{i+1} - y_i)^2}} \\ (1) \quad & - \frac{c}{\rho} dy_i/dt + g + \frac{1}{\rho} f(\tilde{x}_i, t). \end{aligned}$$

Here, $x_0(t) = 0, x_{N+1}(t) = L, y_0(t) = 0, y_{N+1}(t) = 0, 1 \leq i \leq N$, and N is the number of particles discretizing the cable. The forcing term $f(\tilde{x}_i, t)$ is taken to be $\lambda \sin 5\pi \tilde{x}_i \sin \mu t$, where $\tilde{x}_i = i\Delta x/L$ and $\Delta x = L/(N+1)$.

The term ρ denotes the mass per unit length of unstretched cable and the term l the unstretched length of the spring between two point masses. The spring constant is denoted by k and $k = \frac{EA}{l}$, where E is Young's modulus and A is the cross section area. As we double the number of particles in modelling a cable, k is increased by two. The damping coefficient per unit unstretched length is denoted by c and the

acceleration due to gravity by g . Moreover, the notation u^+ is defined as

$$(2) \quad u^+ = \begin{cases} u, & \text{if } u > 0 \\ 0, & \text{if } u \leq 0 \end{cases}$$

Such a nonlinear term comes from the fact that when the cables are stretched, there are restoring forces which are assumed to be proportional to the amount of stretching. However, when they are compressed, there is no restoring force exerted on them.

The main tool for this investigation is a computer, using 2nd order Runge-Kutta method. As the physical parameters of the problem are varied, a lot of new interesting solutions are discovered. Through numerical integration of the initial value problems with various initial conditions, we examine the solutions after sufficiently long time when the transient effect have been eliminated.

The method which proved stable under the usual precautions, is such as halving step sizes and time, and comparing results. To check the accuracy of this scheme, the following is noted. The static deflection, in the absence of time-dependent forcing, of hanging extensible cable is available as analytic formula in the paper [5]. One can also find this deflection by taking equal to zero, and solving the initial-value problems until a steady state is reached.

3. Main Results

We discuss numerical solutions of (1). To study the equation numerically, we will search for periodic solutions in a fairly naive way by solving the initial value problems for various initial values and allowing the solution to run for large time. If there is a unique periodic solution, then it is reasonable to hope that after large time, the solution will have converged to it. We emphasize that we have little interest in the intermediate values of the solution to the initial value problem, only the eventual long-time behavior.

We take the interval of length 1, the total mass 5, unstretched length of cable 1.2, $c=3$, and $EA=19.2$, in all the numerical results. This study is to focus on the system on new periodic forcing $f(\tilde{x}_i, t) = \lambda \sin 5\pi\tilde{x}_i \sin \mu t$, where $\tilde{x}_i = i\Delta x_i$ and $\Delta x = 1/(N + 1)$. We concentrate on long-term motions of the 63-particle case.

In the loaded hanging cable with periodic forcing, all initial conditions give a small amplitude solution over a wide range of frequencies. Only when deflections become large, the non linear effect of non resistance to compression become significant. Large initial condition does not guarantee that the motion with large initial condition converge to small-amplitude motion. We observe a variety of nonlinear motions over a wide range of μ and λ .

In all listed figures, the plots show the last six equally profiles of motions in the final period.

1) The 2-nodal and non-symmetric motion

The first form of nonlinear motion is 2-nodal and non-symmetric motion. At $\mu = 7.8$ and $\lambda = 5$, the 2-nodal and symmetric solution which is of the same approximate period as the forcing term is appeared. And the 2-nodal and non-symmetric motion which is of the same approximate period as the forcing term is appeared at the same forcing parameters. Hence, multiple periodic motions exist for hanging cable. Figure 1 and figure 2 show long-term behavior with $\mu = 7.8$ and $\lambda = 5$.

As λ becomes from 5 to 5.8, amplitude of motion is almost same but motion becomes more non-symmetric for the same μ . As λ becomes from 6 to 8, the motions become more fuzzily.

2) The non-symmetric and asymmetric motion

As λ changes from 7 to 7.8 when $\mu = 6.8$, we observe a typical small-amplitude motion exists. However, even after large time, existence of a small linear motion did not guarantee that the long-term solution of the initial value problem would converge to that motion. This appears at $\mu = 6.8$ and $\lambda = 8$ in the event of large initial displacement.

While small linear motion is two-noded and symmetric, the motion under the large initial displacement is 2-nodal and non-symmetric motion and it moves fuzzily.

From $\lambda = 8$, there exist multiple motions which are 2-nodal. i.e., For small-amplitude initial values, the system converged to a small-amplitude solution. For large-amplitude initial values, the system converged to a large-amplitude non-symmetric solution. Figure 3 and figure 4 show long-term behavior with $\mu = 6.8$ and $\lambda = 8$.

We have seen the linear oscillation, whose amplitude is directly proportional to the amplitude of the forcing term. It is shown at λ from

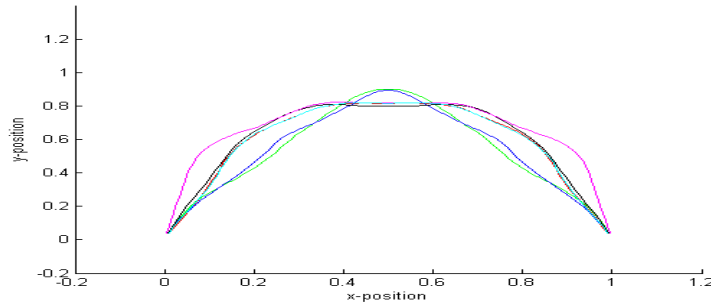


FIGURE 1. The 2-nodal and symmetric motion for $\mu = 7.8$ and $\lambda = 5$.

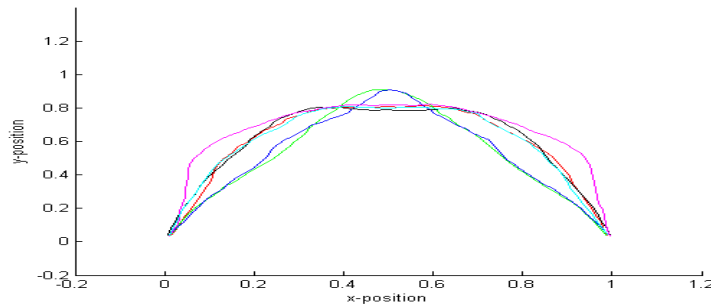


FIGURE 2. The 2-nodal and non-symmetric motion for $\mu = 7.8$ and $\lambda = 5$.

7 to 7.8. However, there also exist large-amplitude motions that are not directly proportional to the amplitude of the forcing term. If we take λ equal to 8, then we find for different initial values, two-nodal but non-symmetric motions as shown in figure 3.

From $\lambda = 8.2$ for the same $\mu = 6.8$, asymmetric 1-nodal motion which moves fuzzily is appeared. Figure 5 shows an asymmetric motion with $\mu = 6.8$ and $\lambda = 8.2$. The great thing about some of the oscillations is the form they take with an asymmetry in the motions, no longer being a oscillation about the mid point but showing a preference for one end. In the motion, as λ changes from 8 to 8.2, motion having bigger amplitude is appeared. Unusual combination of conditions may result in having bigger amplitude. This is shown in figure 5.

Over many different experiments, we found above type of motion occurring, with either end emerging as the preferred end. It seems as

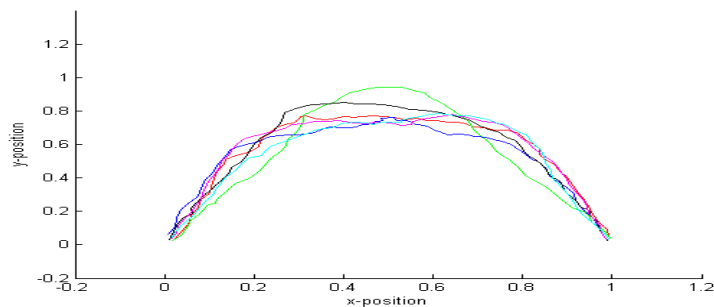


FIGURE 3. The large amplitude motion for $\mu = 6.8$ and $\lambda = 8$.

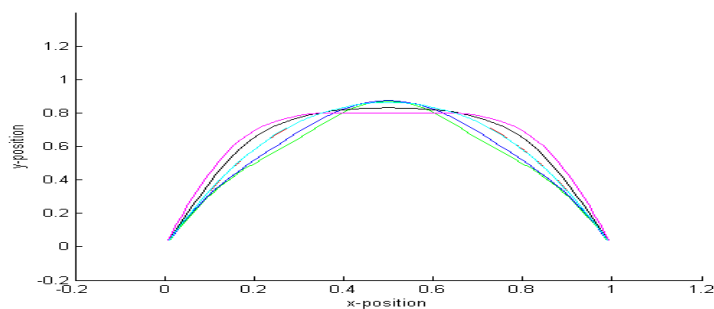


FIGURE 4. The small amplitude motion for $\mu = 6.8$ and $\lambda = 8$.

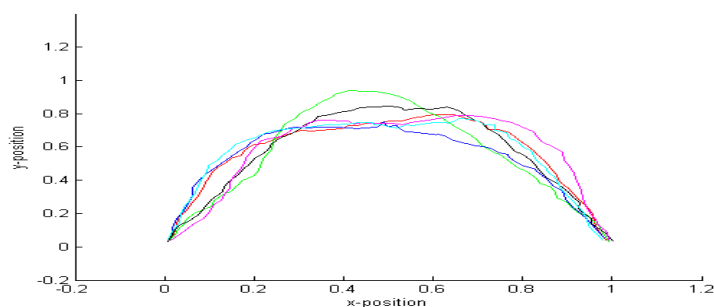


FIGURE 5. The asymmetric motion for $\mu = 6.8$ and $\lambda = 8.2$.

if a form of symmetry breaking occurs, with the symmetric periodic solution presumably becoming unstable. These types of motions exist

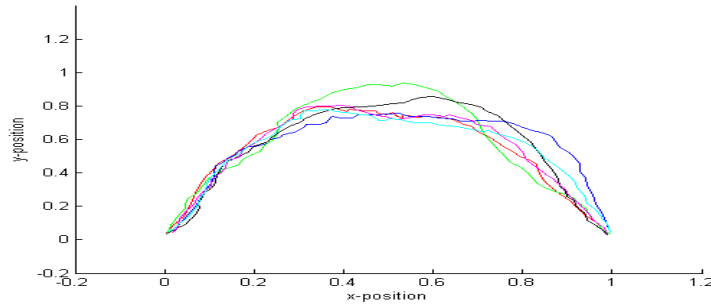


FIGURE 6. The asymmetric motion for $\mu = 6.8$ and $\lambda = 9$.

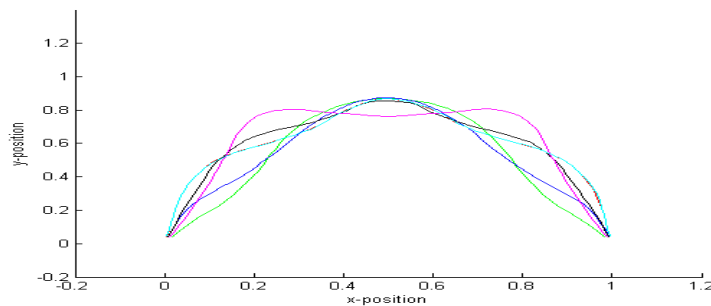


FIGURE 7. The 4-nodal and symmetric motion for $\mu = 8.2$ and $\lambda = 5.8$.

over a wide range of frequency, as shown with $\mu = 6.8$. They coexist over a wide range of amplitude at $\mu = 6.8$, existing from $\lambda = 8.2$ to $\lambda = 9$, essentially independently of λ .

At $\mu = 6.8$, $\lambda = 8.4, 8.6$, and 9 , the greatest oscillation occurs at approximately nine tenth and oscillation occurs quietly at one third along the cable. The large amplitude motion which is close to symmetric instead of asymmetric is appeared at $\lambda = 8.6$. This is similar to figure 6. Figure 6 shows one-node motion at $\mu = 6.8$, $\lambda = 9$.

For the same frequency $\mu = 6.8$, the motion with small initial condition is 2-nodal motion(similar to figure 4). But for the same frequency $\mu = 6.8$, the motion with large initial condition has two types of motions. One is asymmetric and 1-nodal motion, the other is non-symmetric and 2-nodal motion. At $\lambda = 9.4$, there does not exist large amplitude motion which is one nodal but exists large-amplitude motion which is 2-nodal

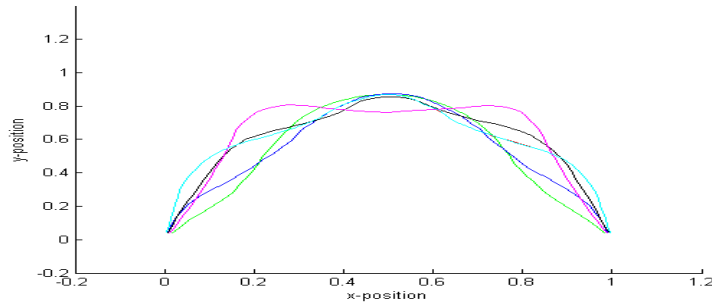


FIGURE 8. The 4-nodal and non-symmetric motion for $\mu = 8.2$ and $\lambda = 5.8$.

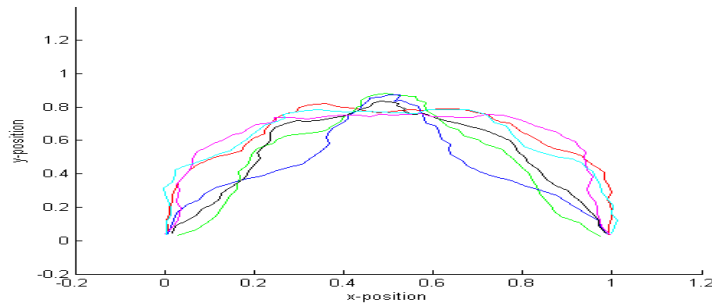


FIGURE 9. The fuzzy and non-symmetric motion for $\mu = 8.2$ and $\lambda = 6$.

motion. At $\lambda = 9.6$, there does not converge to small amplitude motion. For small and large amplitude initial values, the motion converge to a large-amplitude motion.

For the same frequency of the forcing term, as λ becomes large, the magnitude of the small-amplitude motion increases.

3) The 4-nodal and non-symmetric motion

The 4-nodal and non-symmetric motions are appeared at $\mu = 8.2$, from $\lambda = 5$ to $\lambda = 7$. These motions have the same period as the forcing term. Figures of motions at $\mu = 8.2$ show large-amplitude motions which are different from the others. For $\mu = 8.2$, there exist multiple periodic solutions which are symmetric or non-symmetric over a wide range of λ s. The symmetric motions appear only at $\lambda = 5.8$, $\lambda = 6.2$, and $\lambda = 6.4$, for the same μ . At $\lambda = 5.8$, $\lambda = 6.2$, and $\lambda = 6.4$, the motions with

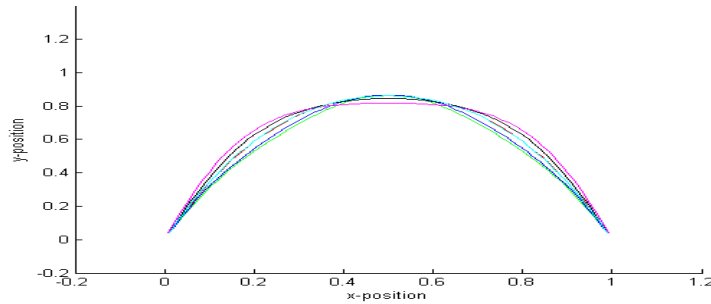


FIGURE 10. The small amplitude solution for $\mu = 7.2$ and $\lambda = 3.6$.

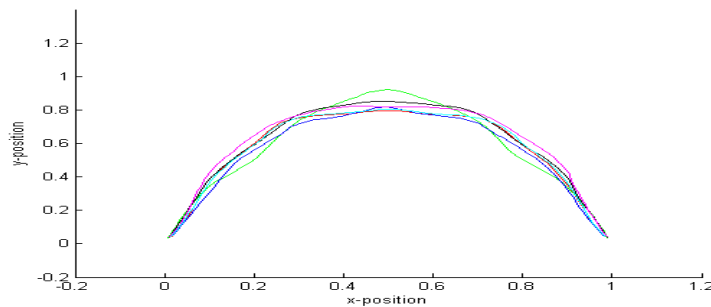


FIGURE 11. The large amplitude solution for $\mu = 7.2$ and $\lambda = 3.6$.

large initial conditions converge to 4-nodal and non-symmetric motions, while the motions with small initial conditions converge to 4-nodal and symmetric motions.

In the motions, as λ changes from 5.8 to 6, more asymmetric motion is appeared. This is shown in figure 8.

Figure 7 shows long-term behavior with small initial condition at $\mu = 8.2$ and $\lambda = 5.8$. For above λ s, the difference between the motion with large initial condition and one with small initial condition is symmetry. They seem to be almost independent of the amplitude of the forcing term.

In the motions, as λ changes from 5.8 to 6, motion which moves more fuzzily and longitudinally is appeared. This is shown in figure 9.

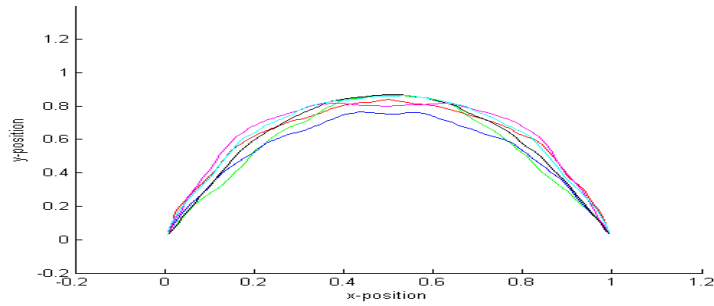


FIGURE 12. The no-nodal motion for $\mu = 7.2$ and $\lambda = 4$.

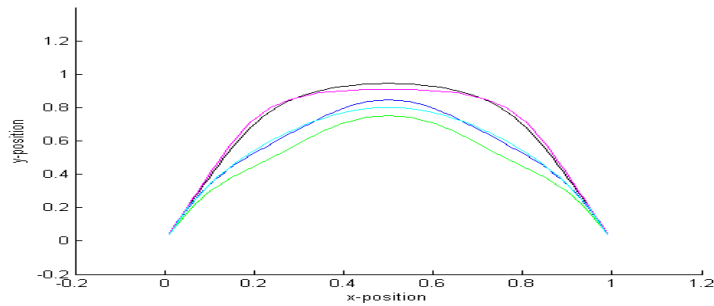


FIGURE 13. The no-nodal motion for $\mu = 5.4$ and $\lambda = 9$.

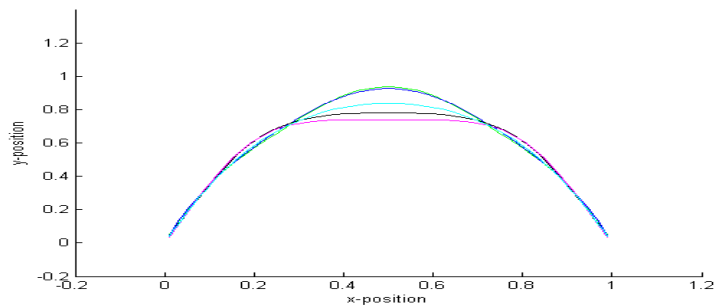


FIGURE 14. The 2-nodal motion for $\mu = 5.4$ and $\lambda = 9$.

4) The 2-nodal symmetric motion

At $\mu = 7.2$ and $\lambda = 3.6$ for the large initial values, the system converges to a 2-nodal symmetric motion which has the same period with the

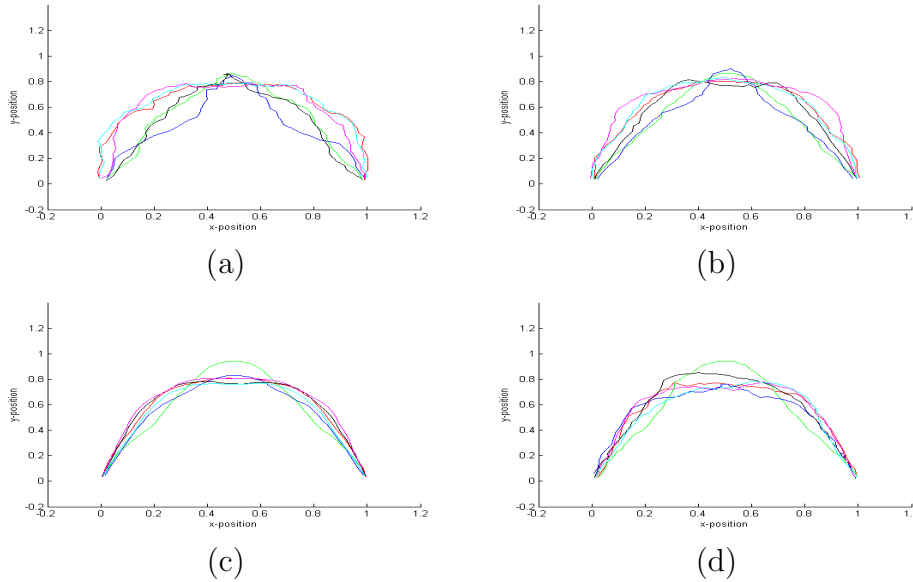


FIGURE 15. The large amplitude motion for (a) $\mu = 8.2$, (b) $\mu = 7.8$, (c) $\mu = 7.2$, (d) $\mu = 6.8$, and $\lambda = 8$.

forcing term. For the same forcing parameters and the small initial values, the system converges to a 2-nodal symmetric motion which is periodic with the forcing term. These are shown at figure 10 and figure 11. Although two figures are 2-nodal, they are different. Hence, multiple periodic solutions exist at $\mu = 7.2$ and $\lambda = 3.6$.

As λ changes from 3.8 to 4, the shape at $\lambda = 4$ is similar to one at $\lambda = 3.8$ but amplitude at $\lambda = 4$ is a little bit large. At $\lambda = 4$, no-nodal motion exists besides two symmetric solutions which are 2-nodal. Figure 12 shows no-nodal motion at $\mu = 7.2$ and $\lambda = 4$. The magnitude of the motion increases and non-symmetry begins to appear from $\mu = 7.2$ and $\lambda = 4.4$. At $\mu = 7.2$, the system converges to a symmetric motion which is periodic over wide range of λ . The fuzziness in 2-nodal motions barely appears over wide range of λ . There exists no-nodal motion which is periodic from $\lambda = 4$. In the motions, as λ changes from 3.6 to 4, motion having bigger amplitude is appeared. This is shown in figure 12.

5) The multiple motions: 2-nodal motion or no-nodal motion
 At $\mu = 5.4$, the system converges to the small linear motion over the wide range of λ . The motion appears to be in a regular oscillation of the frequency with the forcing term which is a standard wave.

However, at $\mu = 5.4$ and $\lambda = 9$ for large initial values, the system converges to a large-amplitude motion which is symmetric and no-node. This is presented in figure 13. At $\mu = 5.4$ and $\lambda = 9$ for small initial values, the system converges to a small-amplitude motion which is symmetric and 2-nodal. This is presented in figure 14. Hence, the system has the multiple motions at $\mu = 5.4$ and $\lambda = 9$. The motions appeared to be of the same period as the forcing term.

We observe that large-amplitude oscillations occur away from the linear resonance. When in large oscillation motions, decreasing the frequency of the forcing term from $\mu = 6.8$ to $\mu = 8.2$ with $\lambda = 8$ may actually increase the amplitude of the oscillation. This is shown at figure 15. This fact was already expected from prior numerical experience with simpler asymmetric systems [7].

4. Conclusion

We consider a nonlinear model in that if we pull on a rope, it resists, and if we push, it does not. We show that this causes large amplitude oscillations that would notably predicted by the linear theory. Although large-amplitude oscillations have smaller amplitude than motions in other study [13], the motions have different nodal structure from small-amplitude oscillations. In fact, different nodal structure was observed prior to the failure of the Tacoma Narrows Bridge.

If λ is very small, then the eventual results for large and small initial data are the same: convergence to the linear solution. For larger values of λ , there is a possibility of convergence to a large- or small- amplitude motion. We investigate the experiment by looking at various types of oscillations which occurred when the value of the frequency is taken to be and we repeat that numerical motions that the motion converged to.

As a result of exhaustive computational experiments, we arrived at the following conclusion:

- Numerical results indicate that the magnitude of the oscillations increases as the frequency of the forcing term is decreased.
- Large-amplitude and small-amplitude periodic oscillations may coexist for the same forcing term and unusual combination of conditions may result in changing from one to the other.
- Asymmetric oscillations occur over a wide range of frequency in the presence of symmetric forcing data, which is by the nonlinear effects.

-Asymmetric oscillations may occur in which the amplitude is quite small at the mid-point but becomes large at points some distance from the mid-point.

-Large symmetric oscillations show a variety of different nodal structure of the motion according to forcing parameters.

Above conclusion shows the nonlinear behaviors of the discrete loaded cable, and it may be correspondence to a mathematical explanation for catastrophic failures of Tacoma Narrow Bridge. We expect that in the future some of these results will have application in the study of electric circuits, where most of the present work treats capacitors as linear.

References

- [1] O.H. Amann, T. von Karman, and G.B. Woodruff, *The Failure of the Tacoma Narrows Bridge*, Federal Works Agency, 1941.
- [2] S.S. Antman, *The Equations for Large Vibrations of Strings*, American Mathematical Monthly, **87** (1980), 359–370.
- [3] F. Bleich, C.B. McCullough, R. Rosecrans, and G.S. Vincent, *The Mathematical Theory of Suspension Bridges*, U. S. Dept. of Commerce, Bureau of Public Roads, 1950.
- [4] J.P. Den Hartog, *Mechanical Vibration*, McGraw-Hill, 1934.
- [5] R.W. Dickey, *The nonlinear string under a vertical force*, SIAM J. Appl. Math. **17** (1969), 172–178
- [6] L.E. Ericsson, *Limit Amplitude of Galloping Buff Cylinders*, AIAA Journal **22** (1984), 493–497.
- [7] J. Glover, A.C. Lazer, and P.J. McKenna, *Existence and Stability of Large Scale Nonlinear Oscillations in Suspension Bridges*, Journal of Applied Mathematics and Physics(ZAMP) **40** (1989), 172–200.
- [8] J.C.R. Hunt and M.D. Rowbottom, *Meteorological Conditions Associated with the Full-span Galloping Oscillations of Overhead Transmission Lines*, Proc. IEEE, **120** (1973), 874–876.
- [9] K.C. Jen, Y.S. Choi, and P.J. McKenna, *The Structure of the Solution Set for Periodic Solutions in a Suspension Bridge Model*, IMA Journal of Applied Mathematics **47** (1991), 283–306.
- [10] A.C. Lazer and P.J. McKenna, *Large-Amplitude Periodic Oscillations in Suspension Bridges: Some New Connections with Nonlinear Analysis*, SIAM Review **32** (1990), 537–578.
- [11] R.K. Mathur, A.H. Shah, P.G.S. Trainor, and N. Popplewell, *Dynamics of a Guyed Transmission Tower System*, IEEE Transactions on Power Delivery, PWRD-2 (1987), 908–916.
- [12] M. Novak, A.G. Davenport, Members, ASCE, and H. Tanaka, *Vibration of Towers due to Galloping of Iced Cables*, Journal of the Engineering Mechanics Division **2** (1978), 457–473.

- [13] Hyeyoung Oh, *Motion in a hanging cable with various different periodic forcing*, J. Korean Soc. Math. Educ. Ser. B: **21** (4) (2014), 281–293.
- [14] A.S. Richardson, Jr. and Steve A. Fox, *A Practical Approach to the Prevention of Galloping in Figure-8 Cables*, IEEE Transactions on Power Apparatus and Systems, PAS-99 (1980), 823–832.
- [15] *Two Recent Bridges Stabilized by Cable Stays*, Eng. News-Record, Dec. 5, 1940, 752–754.
- [16] K. Yusuf Billah, Robert H. Scanlan, *Resonance, Tacoma Narrows bridge failure, and undergraduate physics textbooks*, Am. J. Phys. **59** (2), Feb 1991.

Hyeyoung Oh
Department of Mathematics Education
Incheon National University
Incheon 402-808, Korea
E-mail: hyoh@inu.ac.kr